

# AI 3D Printing Process Parameters Optimization

Park Hong Seok<sup>a</sup> and Nguyen Dinh Son<sup>b</sup>

Department of Mechanical and Aerospace, University of Ulsan, 93-Daehak-ro, Ulsan, South Korea

**Keywords:** Artificial Neural Network, Selective Laser Melting, Ti-6Al-4V, Optimization.

**Abstract:** Optimization parameters of Selective Laser Melting (SLM) process is a significant question currently. Due to attractive advantages, namely high density of printed products and freely design, the SLM has been increasingly applied in industrial manufacturing. However, not only various influenced factors but also their range affects to the printing process. Therefore, it is difficult and requires much testing time and cost to select a suitable process parameter for manufacturing a desirable product. In this article, a supervised learning Artificial Neural Network was applied to build an optimization system for finding out optimal process parameters. Inputs of the system are desirable properties of a product as relative density ratio while outputs are the crucial parameters as laser power, laser velocity, hatch distance, and layer thickness. The developed system is a powerful contribution to industrial SLM manufacturing. By applying the system, it requires less pre-manufacturing expenditure and also helps the printing users to choose approximately process parameters for printing out a desirable product.

## 1 INTRODUCTION

Selective laser melting (SLM) powder bed fabrication is additive manufacturing (AM) that starting from metal powder, allows achieving desirable density products layer-by-layer. Each layer anchors to the previous one as the result of a complete fusion of metal powder obtained by a laser beam. The laser spot moves along a scanning pattern generated and controlled by a CAD model of the part to be built. The schematics representation of typical powder-bed fusion system explained in Figure 1. The strength of the SLM process is possible to create any possible geometry (Srivatsan and Sudarshan, 2015a). Therefore, the SLM is attractive to the aerospace, automotive and other industries for present and future.

Due to its excellent mechanical properties such as good stability, good corrosion resistance, and high specific strength, the titanium alloy Ti-6Al-4V is widely used in many industries (Alcisto et al., 2011). However, its high cost and challenging machinability somewhat restrict its use in conventional manufacturing methods, namely forging and casting (Tan et al., 2018). Nevertheless, the use of Ti-6Al-4V

in SLM offers the benefits of recycling the unprocessed metal powder, geometrical freedom in product design, and time and energy efficiencies (Kruth et al., 2005).

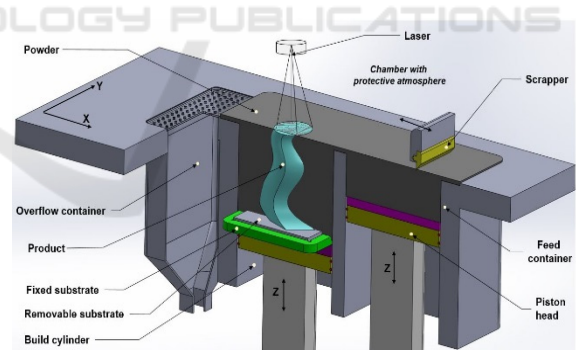


Figure 1: A schematic of a Selective Laser Melting method.

Although an attracting manufacturing method for the aerospace, automotive and other technological industries, printing a desirable product is complicated because of many affected factors and their wide range that significantly impacts on the mechanical properties of the printed product. Many papers have tried to optimize the SLM process. It is evident in all

<sup>a</sup> <https://orcid.org/0000-0002-8382-4843>

<sup>b</sup> <https://orcid.org/0000-0001-7509-3422>

these methods that investigating process parameters independently is incorrect because the printed product quality is a function of the relationship between several crucial process parameters. Therefore, determining the optimal process parameters by applying an artificial neural network to print a desirable density product is the goal of this research.

Artificial neural networks (ANNs) motivated by modeling of human brains and nerve cells are currently considered as one of the neuro-modeling techniques used in associate with robust optimization. Using artificial neural networks to optimize engineering problems has been a great application, such a welding process (Sivagurumanikandan et al., 2018). In SLM, there were some research analysed applying ANNs but individual process parameters (Mertens et al., 2014)(Kempen et al., 2011). In this article, four crucial process parameters as laser power, laser scanning speed, hatch distance and layer thickness are optimized to get a desirable density of the manufactured product.

## 2 METHODOLOGY

The material selected for this study was the titanium-alloy Ti-6Al-4V ELI, Grade 23 (SLM Solutions Group AG, Germany), supplied in powder form with an average particle size of about 20-63 $\mu$ m. An SLM printer (MetalSys150; WinforSys Co., Ltd., Korea) with an IPG ytterbium fiber laser, (YLR-200-AC-Y11; IPG Photonics) 200W maximum output, air-cooled, was used to process the powder. Scanning electron microscope (SEM) image of powder material and particle size distribution were shown in Figure 2a and 2b, respectively. An SLM machine (MetalSys150, Winforsys co., Ltd) with the YLR-200-AC-Y11, IPG Ytterbium Fiber Laser, 200W maximum output, air-cooled, was used to process. Table 1 shows the technical parameters of the SLM printer. The printing process used the meander laser scanning strategy in which the laser scan direction in  $n^{\text{th}}$  layer is perpendicular to that of the  $n+1^{\text{th}}$  layer, which is the same as the  $n-1^{\text{th}}$  layer.

Table 1: Technical parameters of the MetalSys150.

Item	Value
Wavelength	1,075nm
Output power	200W max
Beam quality	M2,1.1
Beam spot	70 $\mu$ m
Building size	150 $\times$ 150 $\times$ 250mm3
Max scanning	7 m/s max

Argon gas was filled into the chamber to maintain oxygen degree at below 0.5 percent. The chamber temperature was at 28 $^{\circ}$ C. The process parameters for experiments are shown in Table 2. Parameters were in the range of settings recommended by the machine manufacturers. After printing, SLM processed parts were tested. A GR-200 analytical balance (A&D Company, Ltd., Tokyo, Japan) was combined with the AD-1653 density determination kit to measure the density of the printed parts based on the Archimedes' principle. The density of the samples is obtained according to the weight of the sample in the air, the weight of the sample in liquid, the distilled water (DI water) and the density of the liquid.

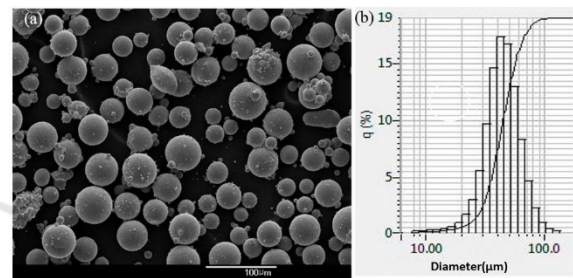


Figure 2: SEM image (a) and particle size distribution (b) of the used material powder.

Table 2: SLM process parameters used for experiments.

Factor	Level		
	80	120	180
Laser power (W)	80	120	180
Laser scanning speed(mm/s)	800	1200	2500
Layer thickness( $\mu$ m)	20	50	100
Hatch distance( $\mu$ m)	35	50	90

### 2.1 Neural Network Parameters

A feedforward ANN includes four input nodes as four process parameters, while output was the density of the printed part. Two hidden layers (Rojas, 1996) with ten, eight nodes (L. Fletcher; V. Katkovnik; F.E. Steffens; A.P. Engelbrecht, 1998) in first, second hidden layer respectively with a full connection.

#### 2.1.1 Data Processing

Significant differences in the values of four investigated process parameters as the inputs and product quality as the output leads complicate the learning process of the neural network. For solving this potential problem, all input and output were previously scaled by using a standardization:

$$z = \frac{x-\mu}{\sigma} \quad (1)$$

With mean:

$$\mu = \frac{1}{N} \sum_{i=1}^N (x_i) \quad (2)$$

and standard deviation:

$$\sigma = \sqrt{\frac{1}{N} \sum_{i=1}^N (x_i - \mu)^2} \quad (3)$$

### 2.1.2 Neural Network Architecture

The number of neurons in the input layer is equal to the number of the investigating parameter. The quantity of hidden layer usually is set between the size of the input and size of the output. Selecting the number of neurons in the hidden layers is very important. One hand, using too few neurons in hidden layer will result the underfitting. On the other hand, too many of them can result in overfitting. There are many methods for determining a suitable number of hidden nodes. In this research, two hidden layers were applied and the number of hidden node was calculated by the following:

$$N_h = \frac{N_s}{(\alpha(N_i + N_o))} \quad (4)$$

$N_i$ : number of input neurons

$N_o$ : number of output neurons

$N_s$ : number of samples in training data set

$\alpha$ : an arbitrary scaling factor usually 2-10

### 2.1.3 K-fold Cross-validation

For training the model, the dataset is usually split into training data and test data. The training dataset includes a known output, and the model learns on this data to be described to other coming data. The test dataset is used to test the prediction of the model. However, splitting data that is required to reflect the essential characteristics of the problem is not easy.

Additionally, by partitioning the available data into other sets, the data will significantly decrease the number of samples which can be used for learning the model, and the results can depend on a particular random selection for the pair of sets. Therefore, in this article, the k-fold cross-validation is applied to solve the mentioned problems. In k-fold cross-validation, the original sample is randomly partitioned into k equal sized subsamples. Of the k subsets, a single subsample is retained as the validation data for testing the model, and the remaining k-1 subsamples are used as training data. The cross-validation process is then repeated k times (the folds), with each of the k subsamples used exactly once as the validation data. The k results from the folds can then be averaged to produce a single estimation (James et al., 2013). The advantage of this method is that all observations are applied for both training and validation, and each observation is used for validation exactly once. In this article, the 10- fold was selected

### 2.1.4 Activation Function

The rectified linear unit (ReLU),  $f(z) = \max(0, z)$ , was used when going from one layer to the next as an active function (Glorot et al., 2011). It is the most popular non-linear function recently because it learns much faster in networks with many layers, typically comparing the others (LeCun et al., 2015). Nevertheless, the sigmoid function,  $f(z) = 1/(1 + \exp(-z))$ , was used as the active function for the output layer because of real-valued output.

### 2.1.5 Neural Network Validation

The ANN was trained by minimizing the mean square error as a loss function with the Adam Optimizer algorithms (Kingma and Ba, 2017). The loss function was the mean absolute error and calculated as:

$$L_0(\mathbf{w}, \mathbf{b}) = \frac{\sum_{n=1}^N |\hat{y}_n - y_n|}{N} \quad (5)$$

Where  $\hat{y}$  and  $y$ ,  $N$ ,  $w$ ,  $b$  are predicted value of the model, experimental output, total of samples, weight, and bias of the neural, respectively.

### 2.1.6 Neural Network Optimization

The Gradient Descent method (Kingma and Ba, 2017) was applied to minimize the loss function by changing the values of the  $\mathbf{w}$  and  $\mathbf{b}$  parameters as the following equation:

$$\theta_{t+1} = \theta_t - \eta \nabla_{\theta} L(\theta_t) \quad (6)$$

In which:

$\theta$ : is a neuron network parameter

$\nabla_{\theta} L(\theta_t)$ : is the derivation of the loss function at a point  $\theta$  at the  $t^{th}$  loop.

$\eta$ : learning rate, 0.05.

### 2.1.7 Dropout

Overfitting is a problem that often happened in machine learning. It is a phenomenon that model is too fit the training data, and it will fit the noise in the data rather than finding a general predictive rule (Tušar et al., 2017). A signal to recognize the overfitting is that training error is small while the testing error is high. For preventing overfitting, the dropout methods were used. Dropout means shutting down units in a neural network (Srivastava et al. 2014) (Dahl et al., 2013) (de Rosa et al., 2018). It temporarily deactivates it from the network. The selection of ignored units is random. Each unit has remained with a fixed probability  $p$  independent of another one. In this research, the probability of retaining a unit in the network was 0.8. After training, at the testing set, the network is used without dropout

in which the weights and biases are scaled as  $W_{test}^{(l)} = pW^{(l)}$ .

## 2.2 Optimization System Algorithm

The Generated Data was created by integrating from four the investigated process parameters, as shown in Table 2. Laser power changes from 80W to 180W with 5W variation. Laser scanning velocity values change between 800mm/s to 2500mm/s with 100mm/s variation. Layer thickness and hatch distance change from 20 $\mu$ m to 100 $\mu$ m and 35 $\mu$ m to 90 $\mu$ m respectively with 5 $\mu$ m variation.

Table 3: Combination of Generated data for predicting.

Factor	Min value	Max Value	Deviation
Laser Power (W)	80	180	5
Laser scanning speed (mm/s)	800	2500	100
Layer thickness ( $\mu$ m)	20	80	5
Hatch distance ( $\mu$ m)	30	100	5

The optimization algorithm is shown in Figure 3 and the following:

1. At the first time, develop an ANN
2. Predicting density ratios from the Generated Data that was created by combining levels of four process parameters. Laser power changes from 80W to 180W with 5W variation. Laser scanning velocity values change between 800mm/s to 2500mm/s with 100mm/s variation while layer thickness and hatch distance change from 20 $\mu$ m to 80 $\mu$ m and 30 $\mu$ m to 100 $\mu$ m respectively with 5 $\mu$ m difference as shown in Table 3.
3. Input a required density ratio of the user that is limited from 75 to 100, in the scope of this paper.
4. Predicted data as the density ratio from the ANN was compared with user requirements.
5. Then process parameters in the Generated Data of which predicted data fit with user needs are indexed.
6. The indexed data were filtered by maximizing the value of the productivity, calculated by:  $\dot{V} = v \cdot h \cdot t$  to point out the optimal parameters. It is a relationship of layer thickness ( $t$ ), laser scan speed ( $v$ ), and hatch distance ( $h$ ).

In this research, ANN implementation, training and the optimization system were developed using the Python programming language, in which the TensorFlow library (Abadi et al. 2016) was applied.

## 3 RESULTS AND DISCUSSIONS

### 3.1 Process Parameters and Printed Part Qualities Relationship

Figure 4 indicates the relationship between individual four process parameters and the density of the manufactured part. Figure 4a shows the influence of laser power on density at 1400mm/s of laser speed and 40 $\mu$ m of hatch distance. Increasing laser power increased the relative density because of sufficient powder molten. Moreover, Figure 4a illustrates the effect of layer thickness. The blue, green, red and black lines present the influence of laser power at 20 $\mu$ m, 40 $\mu$ m, 60 $\mu$ m, and 80 $\mu$ m of layer thickness respectively. It is precise that increasing layer thickness reduces the density ratio.

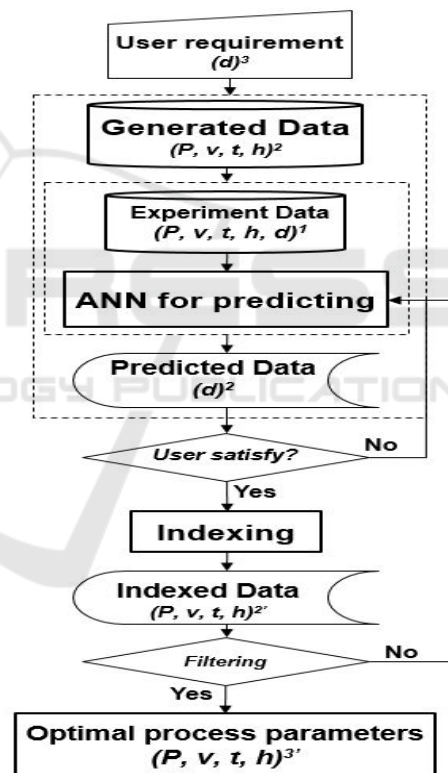


Figure 3: Algorithms for optimization system.

At a specific laser power, a thicker layer material powder will less be moul. Figure 4b presents the effect of laser scanning speed at different hatch distances. It shows a severe incline during increasing laser speed. High scanning speed of laser reduces interaction time of laser spot on material that generates lower densities because of incomplete melting of powder (Cherry et al., 2014). Additionally,

the effect of hatch spaces on density illuminates in Figure 4b. The hatch distance relates to the overlapping area of two adjacent melting lines. Reducing the hatch distance leads over-burning and vaporization within the melting pool. However, insufficient material moulded due to a large hatch distance generated low relative densities. A smaller hatch distance often increases density ratio. However, a combination of low speed of laser scanning velocity and too small hatch space leads balling phenomenon and vaporization that was significantly affected by density (Khan and Dickens, 2012). It explains for a lower density of blue line at 800mm/s compared to others.

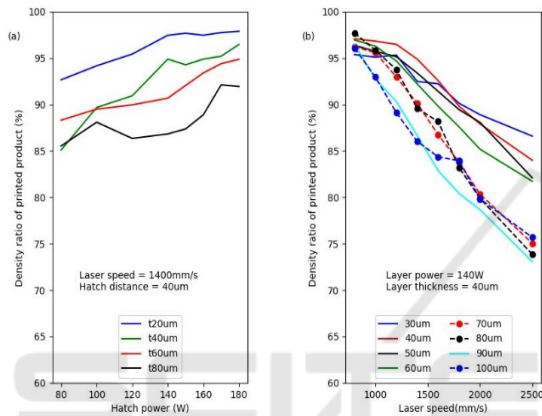


Figure 4: Relationship of individual process parameters and product properties.

### 3.2 Neural Network Evaluation

In order to validate the developed ANN, the mean absolute error (MAE) of the training and testing process is shown in Figure 5. The dark blue line and the orange line present the training and validation of the network. They converge after 3000 epochs. The result elucidates that the network prevents overfitting problem. Additionally, the results show that the maximum error percentage is 1.5% approximately, which is an acceptable value. Therefore, the developed ANN is valid for predicting.

### 3.3 Optimization System Verification

99 percentage of density ratio was used as a request of the user to verify the developed system. Table 4 shows the parameters given by the system. Using the optimal process parameters suggested form the system, a product was printed one more time to confirm the performance of the system. By applying the Archimedes principle, the result indicates 99,8 percentage of relative density. The part was mounted

by hot pressing, polished and examined for porosity. Figure 6 shows a cross-section of the part. Additionally, the optimal parameters confirm a similar result by the response surface methodology (RSM)- based method (Li et al., 2018). It proved the success of the developed optimization system for SLM printing.

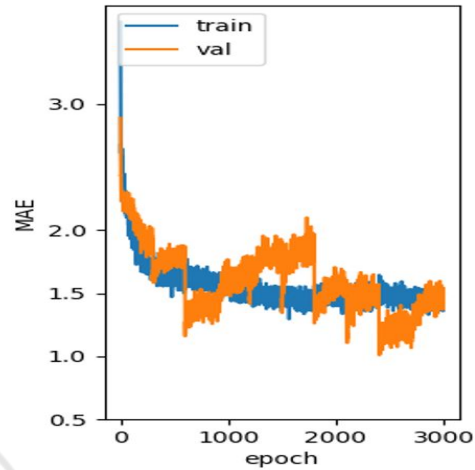


Figure 5: Mean absolute error of training and testing processes of ANN.

Table 4: Optimal process parameter set.

Parameter	Value
Layer thickness, $t$ , ( $\mu\text{m}$ )	20
Hatch distance, $h$ , ( $\mu\text{m}$ )	80
Laser power, $P$ , (W)	180
Laser scanning speed, $v$ , (mm/s)	900



Figure 6: A cross-section of a product manufactured by the optimal process parameters set.

## 4 CONCLUSIONS

In this article, a system combining an ANN for optimizing process parameters to fabricate a desirable

product was developed. A supervised neural network was built for predicting a generated data set. Training and testing data set of the ANN were collected from the experiment. The gradient descent method was applied to minimize the loss function. The dropout technique and k-fold validate were used to prevent the overfitting problem. After building the network, a user requirement was compared with predicted data. Process parameters of which predicted values satisfied with user needs were indexed from the generated data set. In order to achieve the optimal process parameters, productivity was added as filtering conditions finally. In the future, the system will be implemented, and training data will more be collected to achieve more accurate results.

## ACKNOWLEDGEMENTS

This work was supported by the Development of PBF 3D printing analysis SW Technology for manufacturing simulation of metal parts in power generation or shipbuilding project.

## REFERENCES

- Abadi, M., Barham, P., Chen, J., Chen, Z., Davis, A., Dean, J., et al. (2016). TensorFlow: A System for Large-Scale Machine Learning. In *12th USENIX Symposium on Operating Systems Design and Implementation (OSDI '16)*.
- Alcisto, J., Enriquez, A., Garcia, H., Hinkson, S., Steelman, T., Silverman, E., et al. (2011). Tensile properties and microstructures of laser-formed Ti-6Al-4V. *Journal of Materials Engineering and Performance*. SPRINGER.
- Cherry, J. A., Davies, H. M., Mehmood, S., Lavery, N. P., Brown, S. G. R., & Sienz, J. (2014). Investigation into the effect of process parameters on microstructural and physical properties of 316L stainless steel parts by selective laser melting. *International Journal of Advanced Manufacturing Technology*. SPRINGER.
- Dahl, G. E., Sainath, T. N., & Hinton, G. E. (2013). Improving deep neural networks for LVCSR using rectified linear units and dropout. In *ICASSP, IEEE International Conference on Acoustics, Speech and Signal Processing - Proceedings*. IEEE.
- de Rosa, G. H., Papa, J. P., & Yang, X. S. (2018). Handling dropout probability estimation in convolution neural networks using meta-heuristics. *Soft Computing*. ELSEVIER
- Glorot, X., Bordes, A., & Bengio, Y. (2011). Deep sparse rectifier neural networks. *AISTATS '11: Proceedings of the 14th International Conference on Artificial Intelligence and Statistics*.
- James, G., Witten, D., Hastie, T., & Tibshirani, R. (2013). *An Introduction to Statistical Learning* (Vol. 103). Springer-Verlag New York.
- Kempen, K., Thijs, L., Yasa, E., Badrossamay, M., Verheecke, W., & Kruth, J. P. (2011). Process optimization and microstructural analysis for selective laser melting of AlSi10Mg. *22nd Annual International Solid Freeform Fabrication Symposium - An Additive Manufacturing Conference, SFF 2011*.
- Khan, M., & Dickens, P. (2012). Selective laser melting (SLM) of gold (Au). *Rapid Prototyping Journal*.
- Kingma, D. P., & Ba, J. L. (2017). Adam: a Method for Stochastic Optimization. *International Conference on Learning Representations 2015*.
- Kruth, J., Vandenbroucke, B., Vaerenbergh, J., & Mercelis, P. (2005). Benchmarking of different SLS/SLM processes as rapid manufacturing techniques. In *Int. Conf. Polymers & Moulds Innovations (PMI), Gent, Belgium*.
- L. Fletcher; V. Katkovnik; F.E. Steffens; A.P. Engelbrecht. (1998). Optimizing the Number of Hidden Nodes of a Feedforward Artificial Neural Network. In *IEEE International Conference on Neural Networks Proceedings*.
- LeCun, Y. A., Bengio, Y., & Hinton, G. E. (2015). Deep learning. *Nature*.
- Li, Z., Kucukkoc, I., Zhang, D. Z., & Liu, F. (2018). Optimising the process parameters of selective laser melting for the fabrication of Ti6Al4V alloy. *Rapid Prototyping Journal*. EMERALD INSIGHT
- Mertens, R., Clijsters, S., Kempen, K., & Kruth, J.-P. (2014). Optimization of Scan Strategies in Selective Laser Melting of Aluminum Parts With Downfacing Areas. *Journal of Manufacturing Science and Engineering*. ASME
- Rojas, R. (1996). *Neural Networks. Neural Networks: A Systematic Introduction* (Vol. 7). Springer-Verlag.
- Sivagurumanikandan, N., Saravanan, S., Kumar, G. S., Raju, S., & Raghukandan, K. (2018). Prediction and optimization of process parameters to enhance the tensile strength of Nd: YAG laser welded super duplex stainless steel. *Optik*. ELSEVIER.
- Srivastava, N., Hinton, G., Krizhevsky, A., Sutskever, I., & Salakhutdinov, R. (2014). Dropout: A Simple Way to Prevent Neural Networks from Overfitting. *Journal of Machine Learning Research*.
- Srivatsan, T. S., & Sudarshan, T. S. (2015a). *Additive Manufacturing: Innovations, Advances, and Applications*. CRC Press, London.
- Tan, F. B., Song, J. L., Wang, C., Fan, Y. B., & Dai, H. W. (2018). Titanium clasp fabricated by selective laser melting, CNC milling, and conventional casting: a comparative in vitro study. *Journal of Prosthodontic Research*. ELSIVIER
- Tušar, T., Gantar, K., Koblar, V., Ženko, B., & Filipič, B. (2017). A study of overfitting in optimization of a manufacturing quality control procedure. *Applied Soft Computing Journal*. ELSIVIER.